DEVELOPMENT AND CHARACTERIZATION OF A NEUTRON BEAM AT THE BONN ISOCHRONOUS CYCLOTRON

M. Loepke*, R. Beck, S. Neubert, D. Sauerland, University of Bonn, Bonn, Germany

Abstract

The Bonn Isochronous Cyclotron provides light ion beams with a charge-to-mass ratio Q/A ≥ 1/2 and kinetic energies ranging from 7 to 14 MeV per nucleon to one of five experimental sites. It is planned to extend the facility's irradiation and experimentation capabilities by providing a neutron beam at one of the experimental areas in the near future. The neutrons are produced in a thick carbon converter through the deuteron breakup and proton stripping reactions. Protons are stopped in the converter whereas the neutrons' flux and angular energy distribution is optimized by a subsequent copper/tungsten collimator. `Geant4` simulations were done and benchmarked against literature in preparation. The predicted neutron yield is in the order of 10^7 neutrons/s, the beam profile is a circular flat top beam with a FWHM of approx. 4 cm and energy distribution is centered around 10 MeV. The beam profile was measured by using a 2D-Line-Scan with a scintillator with n-gamma discrimination properties. The energy distribution will be measured with activation foils. This contribution gives an overview of the setup and compares the simulated beam profile with experimental measurements.

BONN ISOCHRONOUS CYCLOTRON

In Fig. 1, the accelerator facility of the Bonn Isochronous Cyclotron [1] is shown. Here, five experimental sites are provided with light ion beams with a charge-to-mass ratio Q/A ≥ 1/2; like protons, deuterons or alpha particles and kinetic energies ranging from 7 to 14 MeV per nucleon.

The ion beam, generated by two electron cyclotron resonance sources is subsequently directed through a low-energy beamline below the cyclotron and then injected vertically into its magnetic center using an electrostatic hyperboloid inflector.

The Bonn Isochronous Cyclotron is an isochronous, three sector, azimuthally varying field cyclotron. It features a 120°-symmetry in its azimuthal magnetic field pattern due to its magnet yoke being separated into three hill and valley sectors with 0° spiral angle. In each valley, a broadband dual-gap dee is located, providing an acceleration voltage of up to 40 kV

The beam is extracted to a field-compensated channel in a single-turn extraction, using an electrostatic septum. The extracted beam can either be guided to the high current site, used to produce induced radioactivity in target material, or it is transported to the experimental sites via the high-energy beamline [2]. The installation of the proton irradiation site for high-uniformity radiation hardness tests of Si detectors at beamline C is now complete. In the future low energetic alphas will be used in an Ion Beam Analysis setup at beamline D, employing Rutherford backscattering spectrometry (RBS) and particle induced X-ray emission (PIXE). At beamline F, deuterons impinging on a carbon target are utilized to generate neutrons. A collimator made of tungsten and copper encased in borated polyethylene (PE) is then used to create a directed beam of neutrons. This beamline is currently being commissioned.

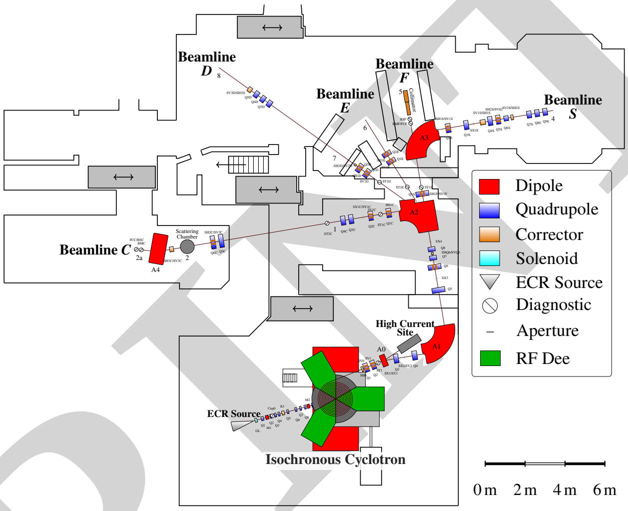

Figure 1: Overview of the accelerator facility.

THE NEUTRON IRRADIATION SITE

The neutron irradation site is located at beamline F. Here, the primary beam is monitored downstream of the A3 magnet with a diagnostic section, consisting of a secondary electron monitor for beam intensity and position monitoring, a pneumatically retractable Faraday cup for its calibration and a pneumatically retractable *Chromox* scintillation screen to monitor the beam profile. The primary beam is then extracted into air through a 30 µm AlMg3 exit Lenard window and onto a neutron production target.

This converter target is thick enough to stop the primary beam. It is mounted at the entrance of a 124 cm long collimator. Figure 2 shows a sketch of the collimator. The inner layer of the collimator consists of tungsten forming an opening cone in the downstream direction. The outer layer is composed of copper acting as a moderator for fast neutrons due to its (n,2n) and (n,3n) cross-sections. The collimator is encased in 30 cm PE, which due to its high hydrogen content further moderates the neutrons' energy through elastic collisions. The PE contains 5% boron, which is a neutron absorber for thermal neutrons due to its (n,α) cross-section.

An enclosure of the irradiation site is neccessary to lower the ambient dose rate in other parts of the facility. Two 50 cm thick concrete walls on the sides of the collimator hold steel

* loepke@hiskp.uni-bonn.de

beams inbetween 13 cm thick borated PE bricks are inserted. On top of this ceiling, another layer of concrete stones is layed out.

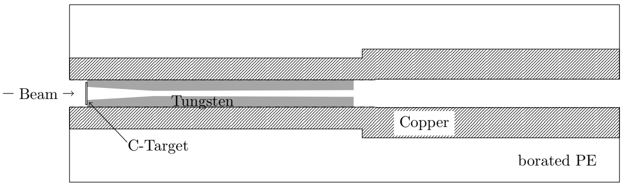

Figure 2: Sketch of the collimator.

NEUTRON BEAM GENERATION

Due to lower maintenance requirements, a solid state target is preferred as converter target over a liquid or gaseous target. Within the operating parameters of the cyclotron, neutron yields from a deuteron beam impinging on a light element target like beryllium, lithium or carbon are higher than from other beam and target combinations.

To estimate and compare the neutron yield and angular distribution of several thick targets, `Geant4v11.0.3` [3–5] as well as the physics list `QGSP_BIC_AllHP` was used, which uses evaluated data and cross-section from the `TENDL`-database for reaction of deuterons below 200 MeV (see Fig. 3). Carbon was choosen as converter target over beryllium and lithium due to its relatively high neutron yield, good mechanical properties and non-toxicity. A 3.1 mm thick graphite target is used. The energy distribution and beam profile of the neutron beam is estimated using `Geant4`.

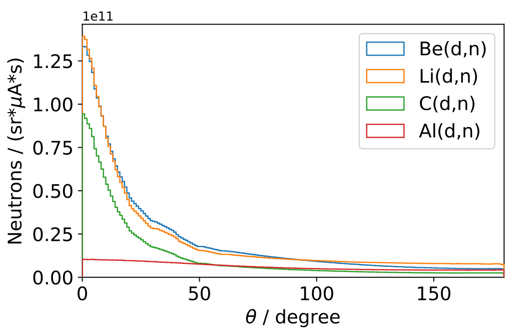

Figure 3: Simulated differential neutron yield for 26 MeV deuterons impinging on different thick targets.

Neutron Beam Profile

The transversal neutron beam profile was determined by measuring an intensity profile generated by transversally moving a scintillator mounted on a photomultiplier tube (PMT) through the expected neutron beam area. Here, the liquid scintillator material EJ309 (an NE213 equivalent) was used to detect neutrons via n-gamma pulse shape discrimination (PSD). PSD is a method to distingush between particles via their pulse shape. I.e. the pulse form generated by a neutron differs from one of a gamma. It is obtained by sampling the charge of every pulse of the PMT with a charge-to-digital converter (QDC) at two set time intervals. A long time interval (100 ns) samples the total pulse charge, while a short interval samples only the first 12.5 ns. By calculating the discrimination value $\frac{\text{long}-\text{short}}{\text{long}}$ and plotting it against long, two structures become visible, which are neutron-induced and gamma-induced events (see Fig. 4).

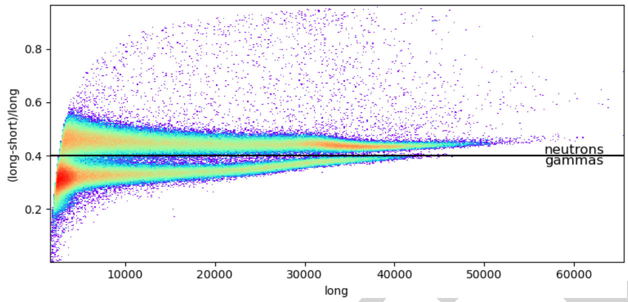

Figure 4: PSD plot of the scintillator being exposed to the beam.

The scintillator with a side length of 2.54 cm was scanned horizontally and vertically through the neutron beam in a meandering pattern, which can be seen in Fig. 5.

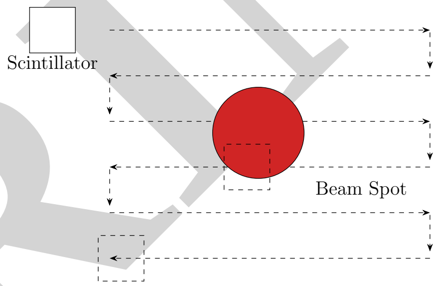

Figure 5: Scanning motion of the scintillator through the beam spot.

Since the scintillator's scale is in the same order as the neutron beam's width, the resulting intensity profile is the true width convoluted with the geometric shape of the scintillator. The original beam profile can be retrieved by means of image restoration. The scintillator can be viewed as a "pixel", creating a "degraded picture" of the beam profile.

In this case, the image degradation can be described with

$$f(x,y) \circledast h(x,y) + \eta(x,y) = g(x,y)\ ,$$

where f is the original, undistorted image, h is the so called point-spread-function of the system (here the geometric shape of the scintillator), $\circledast$ is the convolution operator, η is corrupting Poisson noise and g is the distorted image. Therefore the iterative Richardson-Lucy algorithm [6, 7] can be used to reconstruct the distorted image as

$$\hat{f}_{i+1} = \hat{f}_i \left(h(x,y) * \frac{g(x,y)}{\hat{f}_i(x,y) \circledast h(x,y)} \right)\ .$$

Here, $*$ is the correlation operator and $\hat{f}_i$ is the estimate of f after i-th iterations. Afer each iteration, $\hat{f}$ is re-convoluted with the PSF to obtain the re-distorted image $\hat{g}$. Subsequently $\hat{g}$ and g are compared and the iteration is stopped when the sum of residuals between these two is less than 10^{-3} %. Figure 6 shows the measured distorted neutron beam profile (left) and the reconstructed real neutron beam profile (right). The resulting beam profile is – in agreement with the simulations – a flat top beam. Therefore an elliptical supergaussian function was choosen to describe the data. It can be parameterized as

$$f_{SG} = A \cdot \exp\left[-\left((\frac{x-x_0}{2\sigma_x})^2 + (\frac{y-y_0}{2\sigma_y})^2\right)^n\right] + c\,.$$

Figure 7 shows a supergaussian fit to the reconstructed beam profile and a projection of the reconstructed beam with the fit and the simulation.

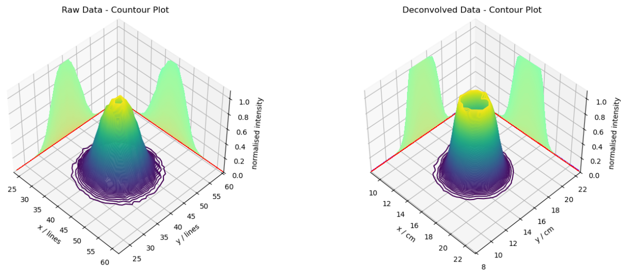

Figure 6: Distorted beam profile taken with the scintillator (left) and reconstructed beam profile (right).

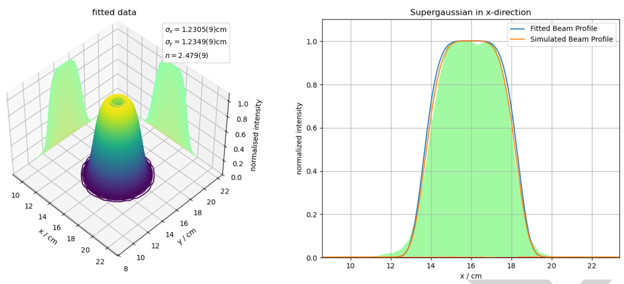

Figure 7: Supergaussian fit of reconstructed beam profile (left) and projection of deconvolved beam profile with a fit to the data and Geant4 simulation result (right).

Neutron Energy Distribution

In the near future, the energy distribution is to be measured to fully characterize the neutron beam. An activation foil based approach is in preparation. Here, a stack of different metallic foils will be exposed to the neutron beam to produce radioisotopes that decay by emitting characteristic γ-rays. By measuring the produced activity in the foils with a high-purity germanium detector and knowledge of the cross-sections of the specific radioisotope production reactions, the neutron energy distribution will be deduced with the GRAVEL algorithm [8]. So far, the expected energy distribution is predicted with a Geant4 simulation (see Fig. 8). It is a broad spectrum reaching up to the deuteron energy E_d with an energy spread around $0.4E_d$.

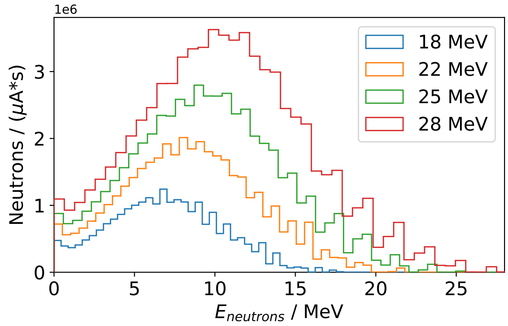

Figure 8: Simulated energy distribution of the neutron beam for different deuteron energies and a thick carbon target.

CONCLUSION

The commissioning of the neutron irradiation site at the Bonn Isochronous Cyclotron is in its final phase. The diagnostic section for the primary beam has been installed and tested. The collimator has been precisely aligned with the beam axis. An enclosing structure of two walls and a ceiling has been build to lower the ambient dose rate outside the area. First measurements of the transversal neutron beam profile have been made and are in close agreement with simulations made beforehand. A measurement of the energy distribution to fully characterize the neutron beam is pending, but preparatory work is already in the progress.

REFERENCES

[1] "The AEG Isochronous Cyclotron at the University of Bonn", *IEEE Trans. Nucl. Sci.*, vol. 13, no. 4, pp. 435–436, Aug. 1966. doi:10.1109/TNS.1966.4324267

[2] D. Sauerland *et al.*, "Status of the Bonn Isochronous Cyclotron", in *Proc. IPAC'24*, Nashville, TN, USA, May 2024, pp. 3539–3541. doi:10.18429/JACoW-IPAC2024-THPR22

[3] J. Allison *et al.*, "Recent developments in Geant4", *Nucl. Instrum. Methods Phys. Res. A*, vol. 835, no. 6, pp. 186–225, 2016. doi:10.1016/j.nima.2016.06.125

[4] J. Allison *et al.*, "Geant4 developments and applications", *IEEE Trans. Nucl. Sci*, vol. 53, no. 1, pp. 270–278, 2006. doi:10.1109/TNS.2006.869826

[5] S. Agostinelli *et al.*, "Geant4—a simulation toolkit", *Nucl. Instrum. Methods Phys. Res. A*, vol. 506, no. 3, pp. 250–303, 2003. doi:10.1016/S0168-9002(03)01368-8

[6] W. H. Richardson, "Bayesian-Based Iterative Method of Image Restoration", *J. Opt. Soc. Am.*, vol. 62, no. 1, pp. 55–59, 1972. doi:10.1364/JOSA.62.000055

[7] L. B. Lucy, "An iterative technique for the rectification of observed distributions", *Astron. J.*, vol. 79, no. 1, pp. 745–754, 1974. doi:10.1086/111605

[8] M. Matzke, "The GRAVEL program", in *Unfolding of Pulse Height Spectra: The HEPRO Program System*, Fachverlag NW in Carl Ed. Schünemannm, 1994, pp. 30–34